

## Analysis of emissivity data from POLEX: Initial results and Development of FASTEM for Arctic Surfaces

Tim Hewison

MRF Technical Note No. 35  
Issue: 2  
27 February 2002

(14 pages)

Controlled Copy Number: - N/A.

	Name	Date	Signature
Document Prepared by	Tim Hewison	30/1/02	
Document Checked by	Jonathan Taylor	30/1/02	
Document Authorised by	Jonathan Taylor	30/1/02	

This document replaces all previous issues

Met Office  
Building Y70, Cody Technology Park  
Ively Road, Farnborough  
Hampshire GU14 0LX, UK

Tel: +44 (0)1252-395781  
Fax: +44 (0)1252-370789  
E-mail: [tim.hewison@metoffice.com](mailto:tim.hewison@metoffice.com)



## Contents

Contents.....	2
1. Aims of this Report.....	2
2. The POLEX-SEPOR experiment.....	2
Instrumentation .....	3
Flights .....	3
3. Emissivity Calculation .....	4
Definition of emissivity .....	4
Modelling down-welling radiances for Deimos .....	4
Correcting atmospheric absorption below the aircraft.....	4
4. Surface Temperature.....	5
Infrared radiometer - Heimann .....	5
Infrared interferometer - ARIES .....	6
Retrieving from microwave radiometer .....	7
5. Surface Classification .....	8
6. Results .....	8
Ice Emissivity Spectra .....	8
Snow and Forest Emissivity Spectra .....	9
Emissivity Gradient between 157-183 GHz.....	12
7. Conclusions, Recommendations and Requests.....	13
8. References .....	14

### 1. Aims of this Report

To improve our understanding of the emissivity of various surface types in the thermal infrared and microwave, MRF have conducted a series of experiments within an ongoing campaign, called ELSIRAM ("Emissivity of Land Surfaces in the InfraRed And Microwave"). This falls within Project RC13B/99 of the Research Plan: "Aircraft interferometer and microwave radiometer studies in support of IASI and AMSU".

This report provides an initial assessment of data analysis from this experiment. It goes on to make recommendations for the future development of the FASTEM model to allow it to more accurately represent the emissivity of a range of surface types found in the Arctic, including multi-year ice. This fulfils the requirements of the milestone in the 2000/2001 Research Plan.

### 2. The POLEX-SEPOR experiment

The application of satellite data from microwave radiometers, such as AMSU, in the arctic is currently limited by our knowledge of the surface emissivity. This is highly variable and difficult to estimate from space-borne observations, due to the uncertainty in the atmospheric absorption and surface temperature.

The Met Office conducted an airborne campaign (POLar Experiment - Surface Emissivity in POLar Regions) in March 2001 based in Tromsø, Norway to measure the emissivity of various arctic surfaces. This experiment was partly funded through the CAATER programme from a proposal by University of Bremen. Their interest is in the validation of total water vapour retrievals over arctic ice. Data is also being analysed by Jeff Ridley and Richard Betts (Hadley Centre) who are interested in the long-wave flux through sea ice and the impact of boreal forest on albedo, respectively.

### **Instrumentation**

Microwave radiometers, known as Deimos and MARSS were operated on a C-130 aircraft. These are total power radiometers, both with a 3 s along-track scan, which includes various views downward, and upward for MARSS. Table 1 summarises their characteristics during POLEX. These instruments are described in more detail in Hewison [1995] and McGrath and Hewison [2001].

Instrument	Deimos		MARSS				
AMSU Channel	1	3	16	17	18	19	20
Frequency (GHz)	24	50	89	157	183±1	183±3	183±7
View Angles (along track)	Down only +35° to -5°		Up and Down +40° to -40°				
Scan Period (s)	3		3				
Polarisation	V + H	V + ~H	Interm.	~V at +40° to ~H at -20°			
Beamwidth (FWHM)	11.0°	11.0°	11.8°	11.0°	6.2°	6.2°	6.2°
Integration time (ms)	50	50	100	100	100	100	100
Sensitivity NEΔT (K)	0.6	0.6	0.5	0.7	0.6	0.4	0.3
Cal. Accuracy (K)	3	3	0.9	1.1	1.0	0.9	0.8

**Table 1 - Characteristics of microwave radiometers operated during POLEX**

The aircraft was also equipped with an infrared radiometer to measure the skin temperature, an infrared interferometer, Short Wave Spectrometer, hemispherical pyranometers and pygeometers, video cameras and a wide range of supporting meteorological sensors.

### **Flights**

Five flights of up to 10 hours duration were flown over various types of arctic sea ice and glaciers in the Svalbard area of the Barents and Greenland Seas. Three of these flights extended to 85° N, to sample first year and multi-year ice, including runs over glacial ice on Svalbard. The other two concentrated on the Marginal Ice Zone. Each flight comprised of a long run at low level (150 m or 600 m), a profile ascent, and a return leg at high level (8.5 km) back along the same track. Dropsondes were released at about 100 km intervals on the return leg to provide atmospheric profiles along the track, which are used to validate the total water vapour retrievals.

On all flights, there was a northerly airflow, which resulted in cloud-free conditions over the ice, but convective cloud developed over open water. The surface temperature got as low as -50 °C, and the surface inversion trapped a variable concentration of ice crystals.

One additional, shorter sortie was flown to measure the emissivity of snow-covered forest. This consisted of a series of low-level runs near Sodankylä in Lapland, northern Finland. The sky was free of cloud in the operating area.

### 3. Emissivity Calculation

#### *Definition of emissivity*

Measured brightness temperatures must be converted to surface emissivity to extend them to general application. However, even the definition of emissivity introduces potential ambiguities unless it is carefully defined. These aspects are discussed below.

This emissivity calculation assumes surface reflection to be purely specular, as this is consistent with the treatment used for the sea surface in fast radiative transfer models, e.g., RTTOV. However, most snow and ice surfaces were close to Lambertian.

The following formula is used to calculate the emissivity using only aircraft data:

$$e(\nu, \theta) = \frac{T_n(\nu, \theta) - T_z(\nu, \theta)}{T_s - T_z(\nu, \theta)} \quad (1)$$

where  $e(\nu, \theta)$  is the emissivity at frequency,  $\nu$ , and incidence angle,  $\theta$ , and  $T_n$  are  $T_z$  the up- and downwelling brightness temperatures, respectively, and  $T_s$  is the surface (skin) temperature. The calculation of each of these terms is discussed below.

#### *Modelling down-welling radiances for Deimos*

Downwelling brightness temperatures at Deimos frequencies are needed to calculate emissivity, but are not directly measured. However, they are not expected to vary significantly. Absorption at 24 GHz is weak due to the very low water vapour levels. Absorption at 50 GHz is dominated by oxygen, which does not vary greatly. Analysis of dropsonde profiles reveals the temperature of the atmosphere above the aircraft remained quite constant during each flight. This allows a single dropsonde to be used to represent the atmospheric profile above the aircraft for each flight. This profile is used as input to a radiative transfer model [Rosenkranz, 1998] to predict the down-welling brightness temperatures that would be measured by Deimos. These values are expected to be accurate to better than 0.5 K.

#### *Correcting atmospheric absorption below the aircraft*

The atmosphere below the aircraft will affect the measured brightness temperatures by absorption and emission (scattering is neglected, as there must be no cloud below the aircraft for surface observation). When calculating emissivity, it is necessary to know the brightness temperatures at the surface, so corrections must be applied to aircraft measurements of both down- and up-welling brightness temperatures.

The atmosphere below the aircraft at any time is assumed to be vertically homogeneous. The average pressure between the flight level and the surface is used. Analysis of the dataset of dropsonde profiles shows that the mean temperature of the atmosphere below the aircraft,  $\bar{T}$ , can be modelled as a polynomial function of the air temperature at the flight level,  $T_{FL}$  and the surface temperature,  $T_s$  (from dropsonde) with an rms accuracy of 0.6 K as :

$$\bar{T} = T_s - 0.26 + 0.519 \cdot (T_{FL} - T_s) - 0.015 \cdot (T_{FL} - T_s)^2 + 0.0013 \cdot (T_{FL} - T_s)^3 \quad (2)$$

The mean humidity of the atmosphere below the aircraft,  $\bar{q}$  can be modelled in a similar way based on the humidity at the flight level,  $q_{FL}$  and the surface,  $q_s$ , assuming it is saturated at the surface (3). This was found to predict  $\bar{q}$  with an rms accuracy of 7%.

$$\bar{q} = q_s - 0.60 \cdot (q_{FL} - q_s) \quad (3)$$

These mean values for the pressure, temperature and humidity of the atmosphere below the aircraft input to a radiative transfer model [Rosenkranz, 1998], which is used to predict the absorption at a single representative frequency for each channel. The frequencies are given in Table 2.

Instrument	Deimos		MARSS				
	1	3	16	17	18	19	20
AMSU Channel							
Effective Frequency (GHz)	23.80	50.07	88.89	157.48	182.38	180.43	176.75

**Table 2 - Representative frequencies used in radiative transfer model**

The atmospheric correction scheme can be validated by examining the observed and corrected down-welling brightness temperatures during a profile ascent in clear skies. This produced an rms difference between the corrected values at 600m and the surface of typically 0.2K for Deimos and 1K for MARSS. The uncertainty introduced in the atmospheric correction scheme dominates the accuracy of the emissivity at 183 GHz from 600m.

The overall uncertainty in the emissivity retrieved from low-level aircraft data by this method is estimated to be  $\pm 0.010$  for  $e=0.900$  at  $183 \pm 7$  GHz. This is dominated by uncertainty in absolute brightness temperatures at the surface, due to the correction for atmospheric absorption.

## 4. Surface Temperature

To calculate emissivity (1), it is necessary to know the surface temperature. This can be estimated in a number of ways described in this section. The resulting emissivity depends on the definition of surface temperature, so it is important to consider the application. In our case, it is to provide a background for retrieving atmospheric information from satellite instruments.

### *Infrared radiometer - Heimann*

The Heimann KT19.82 is a thermal infrared radiometer with a fixed downward view, which it samples continuously at 4 Hz. It is calibrated against an external black-body target, whose temperature is cycled down to -20 °C. However, the calibration process was found to be detrimental to the instrument's agreement with ARIES (see below). Therefore, the uncalibrated data is used in this analysis. Its broad bandwidth (8-15  $\mu\text{m}$ ), shown in Figure 1, provides a "dirty window" in which it measures brightness temperature. Its measurements need to be corrected for atmospheric absorption,  $\tau_{IR}$  which can be modelled as:

$$\tau_{IR} = 0.142 \cdot (\bar{q} \cdot h)^{0.38} \quad (4)$$

Where  $\bar{q}$  is the mean humidity (kg/kg) of the atmosphere below the aircraft from (3), and  $h$  is the aircraft height (m). The coefficients in (4) were derived by regression of the transmittance over the Heimann passband modelled by MODTRAN over a range of high-latitude atmospheres. It was found to predict  $\tau_{IR}$  with an rms of 5%. This scheme typically produces corrections of the order of +1K over open water and -1K over colder ice surfaces from an altitude of 300m in arctic atmospheres. Again, the accuracy of this correction is limited by uncertainty in  $\bar{q}$ , which is estimated to be  $\pm 20\%$  at 300m.

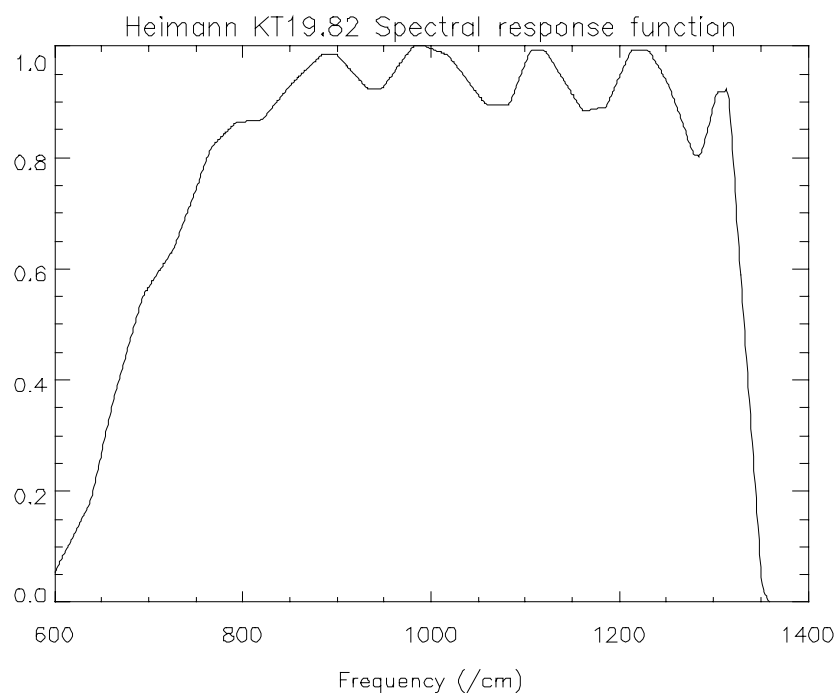


**Figure 1 - Spectral response of Heimann KT19.82**

Strictly, allowance should be made for surfaces with an infrared emissivity of less than 1. This will introduce a bias in the measurement of surface temperature which, in turn, will bias the resultant microwave emissivity. So the brightness temperatures measured by the Heimann need to be further corrected by a factor, which depends on the down-welling infrared flux and the surface emissivity. The infrared emissivity of snow and ice surfaces is the subject for ongoing research [Taylor and Glew, 2001]. Initial results suggest the average emissivity over 800-1200  $\text{cm}^{-1}$  is 0.97 for thick, old sea ice and 0.99 for snow covered land. These figures suggest the skin temperature of sea ice is between 0.2-1.2 K higher than the Heimann brightness temperature (after atmospheric correction). The corrections are correspondingly smaller for snow surfaces. However, these corrections have not been applied to the data, pending confirmation of the infrared emissivity study.

### ***Infrared interferometer - ARIES***

Taylor and Glew [2001] are developing a scheme to retrieve skin temperature and surface emissivity from a combination of up- and down-welling radiance spectra measured in the thermal infrared by ARIES. Initial results show the retrieved skin temperature agrees within  $\pm 1\text{K}$  of the uncorrected brightness temperature measured by the Heimann radiometer over sea ice. It may be fortuitous that the corrections for atmospheric correction and infrared emissivity need for the Heimann tend to cancel out in this case. This has been taken as

validation of the accuracy of the Heimann measurements. These will be used in preference to ARIES retrievals, despite their reduced accuracy, to improve on the sporadic coverage provided by ARIES.

Further analysis is needed of provide validation of the Heimann observations, as well as the atmospheric and emissivity corrections needed to retrieve skin temperature.

### ***Retrieving from microwave radiometer***

Although we can measure the skin temperature using infrared radiometers, microwaves penetrate some distance into snow and ice surfaces. This is due to the weak absorption of microwaves by ice - the imaginary part of its complex permittivity is very low. Snow pack consists of ice crystals suspended in a medium of air. Sea ice is also an inhomogeneous medium - depending on the ice type, it contains air and brine pockets of different sizes. The penetration depth depends on the wavelength, the size and composition of inhomogeneities within the medium. Typically, the penetration depth is ~10 wavelengths in ice, and ~100 wavelengths in dry snow [Haggerty and Curry, 2001] at AMSU frequencies.

Sea ice has low thermal conductivity. Multi-year ice can support a linear temperature gradient of ~50K across a 4 m thickness above water at ~ 1.8 °C. Crudely, 24 GHz will penetrate 1.25 m into the ice, where the temperature is 15K warmer than the surface, but 183 GHz would only be expected to see to a depth where the temperature is 2K warmer than the surface. The thermal conductivity of snow is ~8 times lower than sea ice, but the problem is further complicated by its unknown thickness and the temperature of the underlying surface.

It is possible to retrieve the effective temperature for microwave emissions from MARSS observations. The surface emissivity is assumed to be the same for all 3 channels centred on the 183 GHz water vapour line. This allows simultaneous measurements by these channels to be used to derive the emissivity,  $e(183 \text{ GHz})$  and effective temperature,  $T_{eff}$ . It was found that the emissivity could be derived most accurately from observations in the  $183 \pm 7 \text{ GHz}$  channel due to its weaker atmospheric absorption. The effective temperature was calculated from the  $183 \pm 1 \text{ GHz}$  measurements. These calculations (5) and (6) were initialised using the skin temperature measured in the infrared and iterated until the solutions converged.

$$T_{eff} = \frac{T_n(183 \pm 1 \text{ GHz}) - T_z(183 \pm 1 \text{ GHz})}{e(183 \text{ GHz})} + T_z(183 \pm 1 \text{ GHz}) \quad (5)$$

$$e(183 \text{ GHz}) = \frac{T_n(183 \pm 7 \text{ GHz}) - T_z(183 \pm 7 \text{ GHz})}{T_{eff} - T_z(183 \pm 7 \text{ GHz})} \quad (6)$$

The effective temperature retrieved from MARSS is generally higher than the skin temperature measured by the infrared radiometer by ~18 K over snow covered land, ~12 K over multi-year ice, ~8 K over thick first year, but <~5 K over thin new ice. This difference over multi-year ice is several times larger than expected. It is unlikely to be due to an error in the ice's thermal conductivity, but it is possible to explain a thermal gradient if an exponential temperature profile is adopted. An alternative explanation is that this difference is due to snow cover, which has a very low thermal conductivity. This poses the question: "Can the effective temperature derived from 183 GHz measurements be used in conjunction with IR measurements to retrieve ice thickness or snow depth?".

The effective temperature retrieved from MARSS 183 GHz channels is used to calculate the emissivity for all other MARSS and Deimos channels. Although lower frequencies have a greater penetration depth, this is still felt to be more appropriate than using an IR skin temperature. It has the additional advantage of preventing the emissivity calculated at low frequencies exceeding 1, which is both unphysical and embarrassing. It remains to be seen whether the effective temperature can be retrieved in a similar way from satellite measurements. This would be required to apply the emissivities presented here to the operational assimilation of satellite data.

This has the additional advantage of being insensitive to scattering by small ice crystals often found in the surface inversions. Extinction of this type is difficult to correct for in infrared measurements.

## 5. Surface Classification

It is expected that different surface types will have different emissivity spectra, depending on the mechanisms responsible for emission and scattering. It is therefore necessary to derive a classification scheme which can be applied in the analysis of flight data and to satellite data for use in NWP. The later may require exploitation of NWP fields or other satellite observations.

From the aircraft some surface types are easily classified by visual observation: open water, different forms of new ice, consolidated first year ice and the presence of forestry on snow covered land. In the last case, it is possible to automate the classification based on albedo measured from the aircraft's pyranometers, as described in Hewison and English [1999]. It is also possible to observe clues to indicate the presence of multi-year ice from low-level.

However, it is not easy to identify the presence of snow cover on ice by eye. However, it may be possible to do so by exploiting the different optical characteristics in the visible and near infrared. Briegleb *et al.* [2002] reports the visible albedo of bare ice to be 0.78, increasing to 0.98 for dry snow, while the albedos in the near infrared are 0.36 and 0.70, respectively. These albedos can be derived from upwelling measurements made with the aircraft's Short Wave Spectrometer and modelled down-welling fluxes, which should accurate to 10% in clear skies with low solar elevations. Initial results using the aircraft's pyranometers show this is a promising method to allow the effect of snow cover on emissivity to be investigated.

## 6. Results

### *Ice Emissivity Spectra*

The surface types have been classified manually for two arctic sea ice flights so far. The resulting emissivity spectra for each sample are shown in Figure 2 and Figure 3. The mean and standard deviation of the emissivity is plotted at each frequency. The mean values are connected by a line to illustrate the trend. Each individual observation within each sample is also plotted as a point, with artificial noise applied to the x-axis to illustrate the distribution.

The emissivity in Figure 2 is calculated using the skin temperature derived from the Heimann infrared radiometer (after atmospheric correction). This often results in  $e > 1$ , which is unphysical. Figure 3 shows the emissivity spectra re-calculated using the effective temperature derived from the MARSS' 183 GHz channels. This tends to reduce the emissivity, as it is generally lower than the IR skin temperature, especially where the ice is older, colder or thicker.



Also shown on the plots in Figure 2 and Figure 3 are the emissivity spectra for different surface types, based on the FASTEM model coefficients given in Hewison and English [1999]. The highest solid, straight line represents *Bare New Ice*, the dotted curve *First Year Ice*, the dashed curve *Compact Consolidated Pack Ice*, and the lowest dash-dot curve is *Fast Ice*. These coefficients were derived from emissivities calculated using an IR skin temperature, so only direct comparison with Figure 2 is appropriate. There are several interesting results:

- The emissivity at 183 GHz is consistently higher than at 157 GHz for all surface types. This frequency range probably represents a transition in the scattering efficiency of particles with the surface media. This is an encouraging result, as it would allow the emissivity at one frequency to be parameterised in terms of measurements at the other - for example in the total water vapour retrieval algorithm based on these channels under development at the University of Bremen.
- First Year Ice (FYI) shows a gradual transition along the track of both flights, due to changing physical characteristics of the sea ice or its snow cover. In general, it is best represented by the *Compact Consolidated Ice* classification reported for Baltic Sea ice observations in Hewison and English [1999], however, the emissivity of FYI consistently increases above 157 GHz.
- The last 4 samples for flight A827 show a gradual transition from First to Multi-Year Ice (MYI), as the ice becomes thicker and more porous. These samples included a mixture of old floes with well weathered ridges and younger, ridged pack ice more typical of that seen on other flights (FYI). The last of these is the 'purest' sample of MYI (concentration estimated at 80%). It shows a very similar spectrum to the Baltic *Fast Ice* and quite different from FYI.
- Different glaciers were over-flown on both flights. Their emissivity spectra are quite unlike any other surface type, but depend on the physical structure and temperature gradients within the ice. This implies their emissivity cannot be represented by a global set of coefficients.

### ***Snow and Forest Emissivity Spectra***

Albedo measurements were used to classify the surface types during flight A826 near Sodankylä, Finland. Areas where the albedo was greater than 0.75 were classified as *Deep, Dry Snow*. When the albedo was less than 0.25, it was classified as *Close Forest + Snow*. These are the same thresholds used in Hewison and English [1999].

The resulting emissivity spectra are also shown in Figure 2 and Figure 3 at nadir incidence. The dashed curves on these plots indicate the FASTEM model coefficients for each classification based on observations made in the same area at the same time of year in 1997. The POLEX measurements have quite different characteristics: the emissivity is much higher at low frequencies, and does not increase until 183 GHz. This is due to different physical structure of the snowpack. Although the earlier measurements were classified as *Deep, dry snow*, the temperature had been close to 0 °C a few days earlier and some layers of refrozen snow could have formed below the surface. Such features have a strong impact on the emissivity. This makes it difficult to prescribe a fixed emissivity spectrum for snow. However, again the increase from 157 to 183 GHz is consistent, offering hope that it may be possible to retrieve the emissivity from satellite measurements.

The emissivity of the snow covered forest classification is found to be equivalent to a 45:55 mixture of the dry snow emissivity spectrum measured for this flight and an emissivity of 1 to represent dense conifer forest with no snow cover.

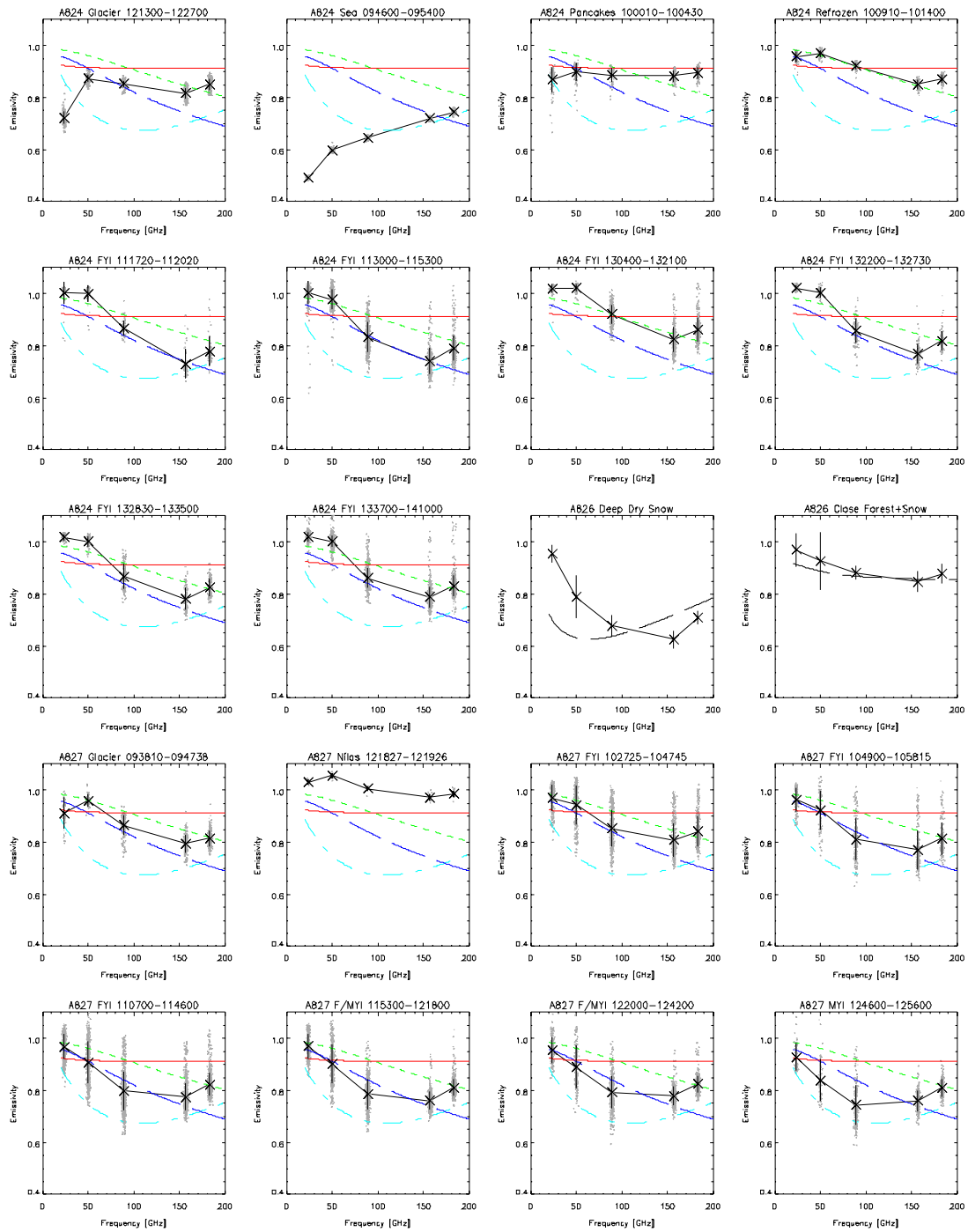


**Figure 2 - Emissivity for POLEX flights A824, A826, A827 calculated from IR Skin Temperature Lines for ice types are FASTEM coefficients from Hewison & English [1999] for Bare New Ice (solid), First Year Ice (dotted), Compact Consolidated Pack Ice (dash) and Fast Ice (dash-dot). For Deep Dry Snow and Close Forest+Snow classifications, FASTEM is shown as dashed lines.**

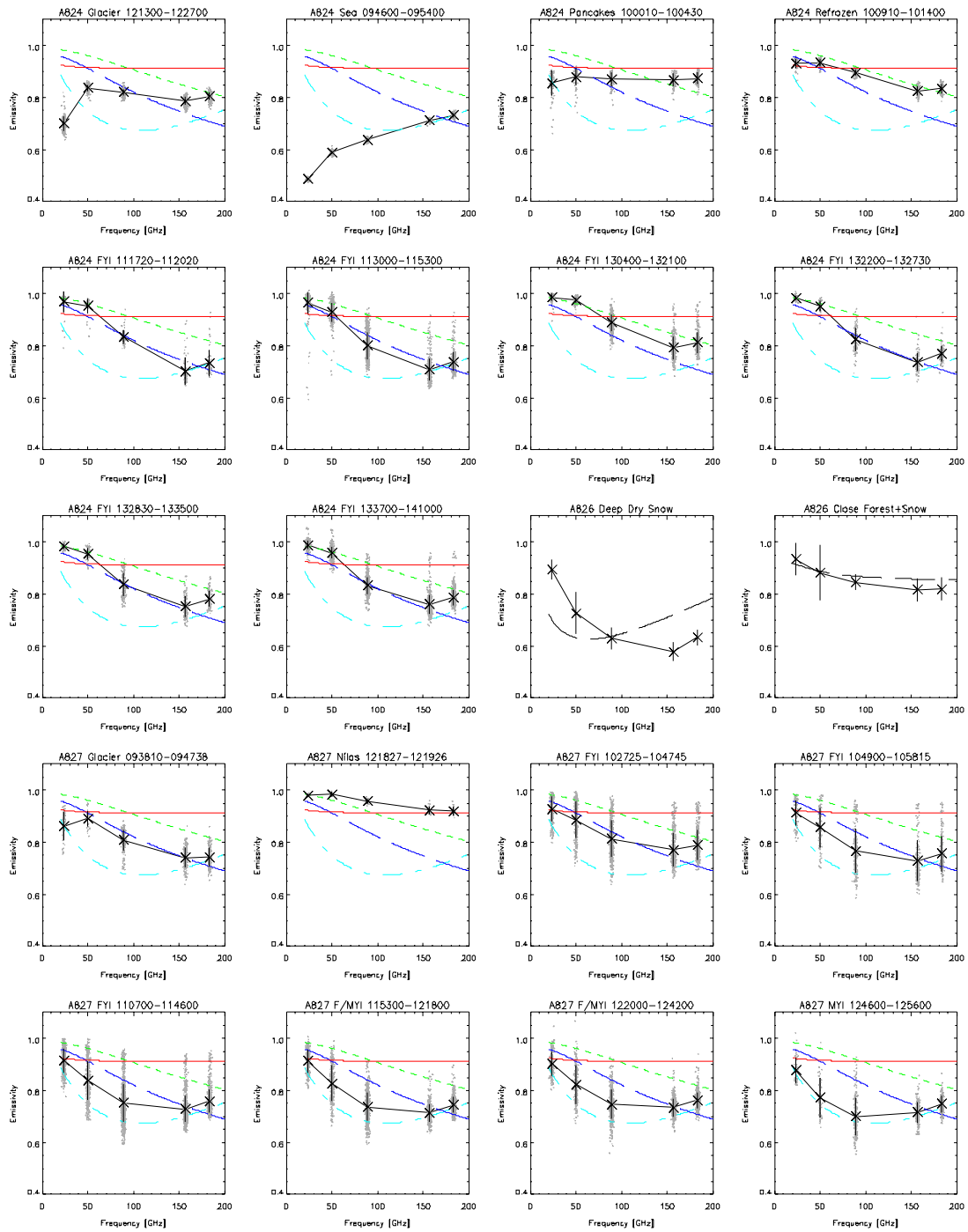


**Figure 3 - Emissivity for POLEX flights A824, A826, A827 calculated from Effective Temperature derived from 183 GHz microwave radiometer measurements.**  
**Lines for ice types are FASTEM coefficients from Hewison & English [1999] for Bare New Ice (solid), First Year Ice (dotted), Compact Consolidated Pack Ice (dash) and Fast Ice (dash-dot). For Deep Dry Snow and Close Forest+Snow classifications, FASTEM is shown as dashed lines.**

### ***Emissivity Gradient between 157-183 GHz***

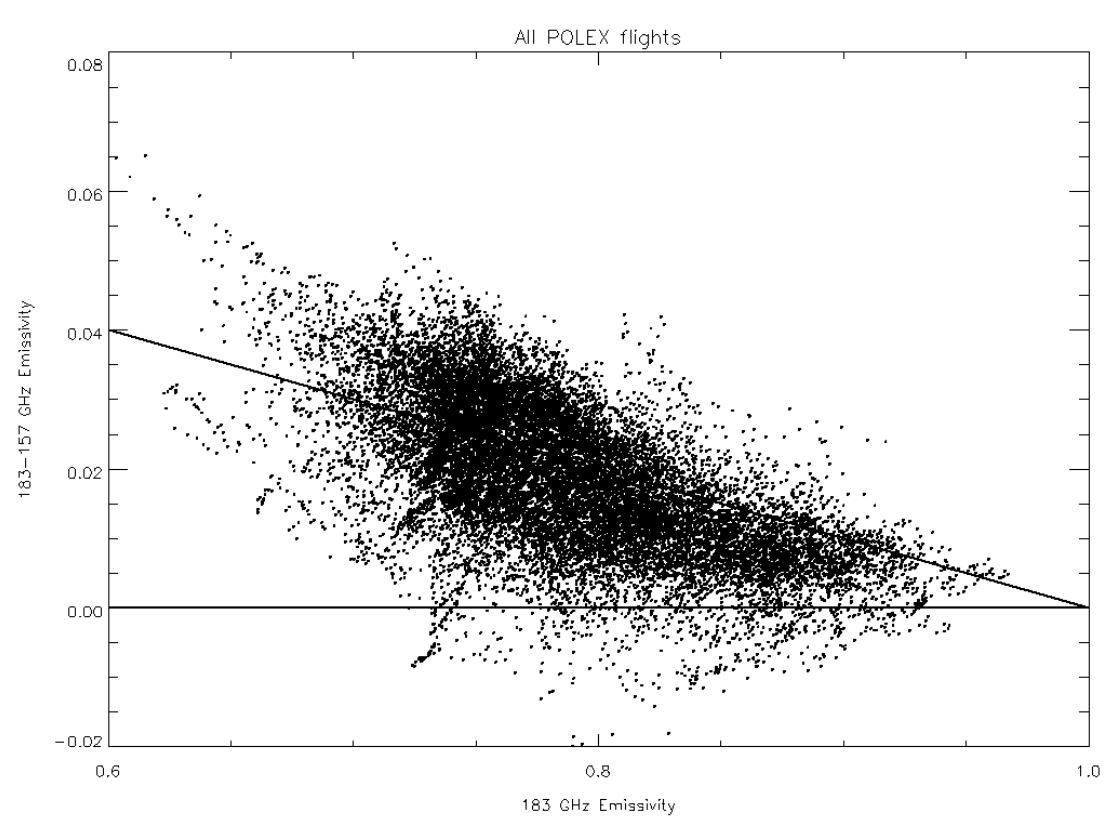


**Figure 4 - Emissivity difference 183-157 GHz for all low-level POLEX data, smoothed over 10 km. Lines show no difference and a 10% difference in reflectivity.**

The emissivity at 183 GHz appears to be consistently higher than at 157 GHz for all surface types overflown during POLEX. This is illustrated in Figure 4. If this is generally true, it would be possible to parameterise one in terms of the other. This would be advantageous for algorithms to retrieve total water vapour using these channels. It may even be possible to retrieve the emissivity at 183 GHz from satellite data. This will be investigated in future work. Also, if the emissivity gradient in this part of the spectrum is approximately linear, this supports the assumption that the emissivity is the same for each of the 183 GHz channels.

## 7. Conclusions, Recommendations and Requests

This initial analysis of data from the POLEX experiment has highlighted a number of problems in the application of the existing fast emissivity model (FASTEM) to arctic surface types:

- The emissivity of sea ice varies over large scales according to its physical characteristics.
- The emissivity of snow is very sensitive to changes in the structure of the snowpack.

These makes it difficult to prescribe an emissivity spectrum to a particular surface type. However, above 100 GHz, the emissivity is less variable and shows a consistent trend. This provides hope that the emissivity in this band could be retrieved from satellite data. This is the subject of ongoing research by Nathalie Selbach at University of Bremen.

Other forthcoming analysis expected to be completed by June 2002:

- Investigate the impact of snow cover on surface emissivity and effective temperature
- Investigate potential of retrieving vertical temperature gradient over ice by flux balancing method. This work is being done in conjunction with Jeff Ridley (Hadley Centre).
- Calculate emissivity for other view angles and polarisations. So far it's only done in nadir.
- Investigate potential of alternate forms of expressing the variation of complex permittivity with frequency. FASTEM currently uses a Debye function, which is incapable of representing non-monotonic changes, which are consistently observed in this dataset. Alternatives should be able to represent resonant absorption, such as a "sloping Gaussian" or "double Debye" function. The chosen function should remove the need to include the additional "surface scattering" term.
- Generation of coefficients to represent these surfaces in a fast emissivity model.

However to proceed, the following decisions are needed from Satellite Applications:

- Confirm whether the specular definition of emissivity is appropriate.
- State a preference for the definition of surface temperature - retrieved from observations at 183 GHz, or from IR skin temperature. If the latter, then the question of whether to include an IR emissivity correction also needs to be addressed.

## 8. References

**B.P.Briegleb et al., 2002:** "Description of the Community Climate System Model Version 2 Sea Ice Model", NCAR Draft report, dated 18/1/2002.

<http://www.cgd.ucar.edu/~bruceb/documentation/documentation.pdf>

**J.A.Haggerty and J.A.Curry, 2001:** "Variability of sea ice emissivity estimated from airborne passive microwave measurements during FIRE SHEBA", Journal of Geophysical Research, Vol.106, No.D14, pp.15265-15277, July 2001.

**T.Hewison, 1995:** "The Design of Deimos: A Microwave Radiometer with Channels at 23.8GHz and 50.3GHz for the UK Met. Research Flight C-130 Aircraft", Proc IGARSS'95, 1995, pp.2261-3.

**T.J.Hewison and S.J.English, 1999:** "Airborne Retrievals of Snow and Ice Surface Emissivity at Millimetre Wavelengths", IEEE Trans. Geosci.Remote Sensing, Vol.37, No.4, 1999, pp.1871-1879

**A.J.McGrath and T.J.Hewison, 2001:** "Measuring the accuracy of a Microwave Airborne Radiometer (MARSS)", Journal of Atmospheric and Oceanographic Tech., Vol.18, No.12, 2001, pp.2003-2012.

**P.W.Rosenkranz, 1998:** "Water vapor microwave continuum absorption: A comparison of measurements and models", Radio Science, Vol.33, No.4, pp.919-928, 1998.

**Jonathan P. Taylor and Martin D. Glew, 2001:** "Retrieving Land Surface Temperature and Emissivity from ARIES data", MRF Technical Note No.36, 2001, Met Office.